

BACKGROUND SUBTRACTION PRACTICE
IN X-RAY REFLECTIVITY RECIPROCAL SPACE MAPPING
AND ITS INFLUENCE ON THE STRUCTURAL PARAMETERS
OF THIN FILMS

© 2012 A. Fouzri, F. Salah, N. Mtiraoui, B. Harzallah, M. Oumezzine

*Laboratoire Physico-chimie des Matériaux, Unité de Service Commun de
Recherche "High resolution X-ray diffractometer", Département de Physique,
Université de Monastir, Faculté des Sciences de Monastir
Avenue de l'Environnement, 5019, Monastir, Tunisia
E-mail: Fouzri.Afif@gmail.com*

Received February 14, 2011; in final form, April 3, 2011

Background subtraction practice in X-ray reflectivity reciprocal space mapping (XRRSM) is described and compared to the traditional specular reflectivity. XRRSM allows determining a more precise contribution of background to the reflectivity signal which manifests itself in an improvement of the resolution of interference fringes. Data analysis and influence of background subtraction determined by two methods on the structural parameters of thin film are discussed using simulated X-ray reflectivity.

1. INTRODUCTION

Grazing-incidence reflectometry using neutrons or X-rays is nowadays a well-established technique for the study of nanoscaled structural properties of thin films using high-intensity sources at synchrotrons or neutron reactors, and also using laboratory X-ray equipment thanks to the rapid development of new optical devices such as bent multilayer [1–4].

It constitutes an excellent non-destructive method of analysing thin layers by the determination of interfacial roughness and the thicknesses of the various layers with high accuracy.

Experimental setup and data reduction for reflectivity experiments are, in contrast, not well discussed in the open literature, possibly because they are considered to be not too different from those used in single-crystal diffraction and especially powder diffraction [5]. It appears that nearly each laboratory working in this field has developed its own methods and data reduction programs without a common adopted practice, such as the one used in the single-crystal community.

The comparison of the results published in the various journals is difficult because the absence of standardization for data reduction in reflectivity experiments. The detailed analysis of the reduction of the data described very recently [6] constitutes a first step in this direction.

Reciprocal Space Mapping (RSM) is a technique of reference for the characterization of epitaxial thin

layers which makes it possible to separate various effects acting in various directions of reciprocal space. We have transposed Reciprocal Space Mapping (RSM) which was developed initially for single crystals and then for the study of epitaxial layers (semiconductors), to the reflectometry measurement of a thin layer.

We will report in this paper the experimental setup and how the background subtraction, as described very recently [6], can be applied to X-ray reflectivity reciprocal space mapping (XRRSM). The influence of background subtraction on the layer thicknesses and interface roughness parameters determined from raw and corrected specular reflectivity measured on the sample glass/gold/cobalt/gold is also discussed.

2. X-RAY REFLECTIVITY RECIPROCAL SPACE MAP COLLECTION STRATEGY

X-ray diffractometry (XRD), and especially reciprocal-space mapping (RSM), are widely used for the analysis of the structural characteristics of epitaxial thin layers. This measurement is based on the complete evaluation of the distribution of intensity around the reciprocal lattice point.

Information concerning the defect structure of the sample in both in-plane and out-of-plane direction can be recovered by analysing the shape of the diffraction profiles. Unfortunately line broadening effects acting in different directions can hardly be separated by running θ – 2θ scans or rocking curves with conventional diffractometers because for each incident angle

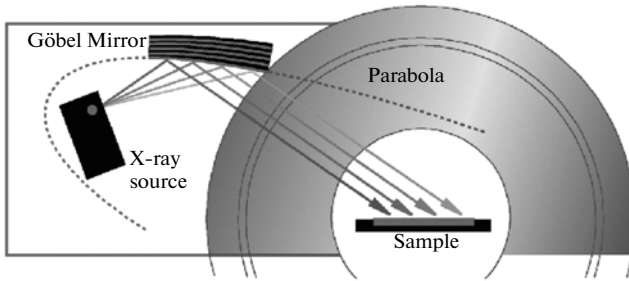


Fig. 1. Schematic illustration of X-ray tube, Göbel mirror and sample with beam path (extracted from D8 X-ray diffractometer user's manual).

the investigated reciprocal lattice point (RLP) is integrated over the Ewald sphere [7]. This problem can be solved by recording the two-dimensional intensity distribution contained in the RLP, i.e. a reciprocal space map.

RSMs are generally recorded with triple- or multiple crystal diffractometers [7] or with modified double crystal diffractometers [8]. In the present study XRD measurements were carried out on a D8 Discover Bruker AXS diffractometer using point detectors equipped with an Eulerian cradle which provides five motorised movements and a Göbel mirror. It is a parabolic mirror consisting of a Ni/C multilayer. This mirror transforms the divergent beam coming from the X-ray tube (Cu) into an almost parallel beam free of K_{β} radiation (Fig. 1) [9]. In addition, the Göbel mirror gives a remarkable intensity gain because the mirror can capture a large solid angle of X-rays leaving the source. Therefore Göbel mirror is a suited optical component for reflectivity measurement.

The method of measurement of a RSM for a given reciprocal lattice point is explained and illustrated for example by Boulle et al in their paper [10].

In our case, we transposed the reciprocal-space mapping to measure the reflectivity of thin layers by carrying out a map $I = f(\omega, 2\theta)$ around the origin of the reciprocal space. The XRRMS are two-dimensional scans $2\theta/\omega$ starting with ω regularly incremented evaluated to trace an area of the reciprocal space. Figure 2 shows an example of variation fields of scans $2\theta/\omega$ and rocking curves ω such as defined in the XRDwizard software.

3. BACKGROUND DETERMINATION STARTING FROM X-RAY REFLECTIVITY RMS

The data reduction falls into several independent stages some of which are closely connected with the way the measurements have been performed and the exact experimental setup. In this section we have applied and compared the data reduction practice as de-

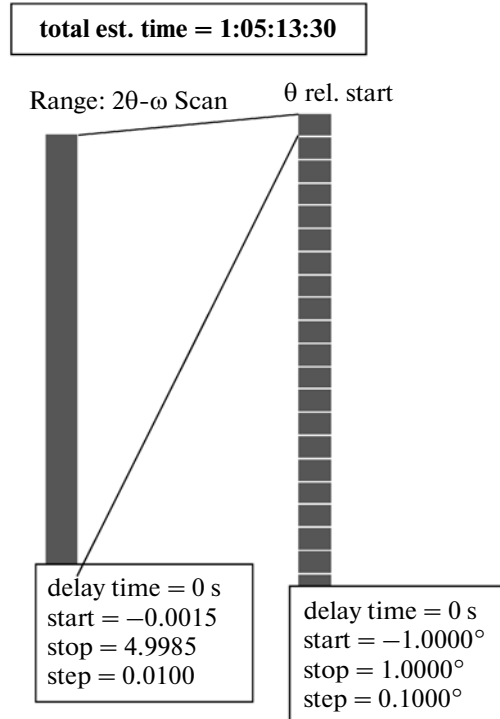


Fig. 2. Example of parameter acquisition of the X-ray reflectivity reciprocal space mapping.

scribed by F. Salah et al. [6] in X-ray reflectivity reciprocal space map. It will show the advantages which of X-ray reflectivity RMS in the subtraction of the background noise compared to the measurement of the traditional specular reflectivity on a layer of cobalt between two layers of gold deposited by electron beam evaporation on a glass substrate.

The determination of the background in reflectivity is completely different with respect to that in single-crystal or powder diffraction. In reflectivity the measured signal in the specular condition consists of the true specular signal plus the background, where it originates from different sources, such as detector noise, air scattering or sample-related diffuse scattering. Subtracting the background is important since it affects the values of the roughness parameters determined from the experiment.

In [6], authors have used two methods to measure the background. The first method is to perform a so-called "offset" scan, i.e. the signal is measured just parallel to the specular ridge. In an angular-dispersive experiment, the offset scan is a so-called $\theta + \delta\theta/2\theta$ scan. Figure 3 depicts how the scan is performed in momentum space; the scan subtends an angle of $\delta\theta$ with the specular scan.

The choice of $\delta\theta$ is, of course, also arbitrary. It is in general determined by performing several rocking or

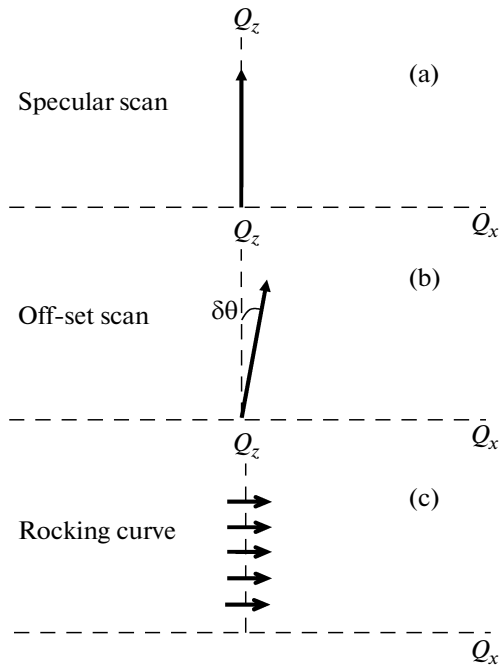


Fig. 3. Scan directions in momentum space for specular scans (a), off-set scans (b) and rocking curves (c). \bar{Q}_x and \bar{Q}_z are components x and z of the diffusion vector \mathbf{Q} .

transverse scans, i.e. keeping the detector fixed while rocking the sample through the specular ridge, and setting the optimal value for $\delta\theta$ as the point where the background is believed to start.

A second method for determining the background consists in performing rocking curves at regular points along the specular ridge, fitting the rocking curves with, for example, a Gaussian profile and using it to determine background parameters for the correction of the measured signal in order to obtain the true specular signal. The true specular signal is subsequently used for data fitting. These authors have measured the background contribution separately.

The sample size $20 \times 15 \text{ mm}^2$, which is relatively large, we cannot neglect sample curvature which could hamper seriously the data reduction. We have used beam knife-edges (Fig. 4) that reduce the air scattering and the beam footprint, so that on the one hand unwanted effects due to a possible substrate curvature are limited, and on the other hand the spill-over angle is reduced then the plateau of total external reflection becomes more visible. In addition the roughness values are lower than 3 nm which suggest that off specular scattering is relatively small and this was also not observed in off scans, so that subtraction of the background scattering is relatively straightforward [6].

The X-ray reflectivity RMS measurement gathers the specular signal, different off specular and rocking curves at

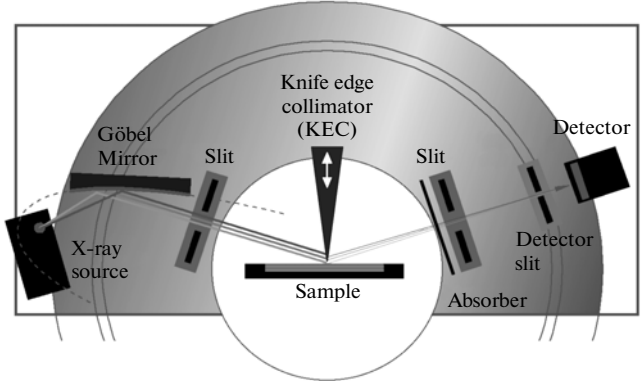


Fig. 4. Experimental setup for X-ray reflectivity (extracted from D8 X-ray diffractometer user's manual).

regular points. We represent in Fig. 5 the X-ray reflectivity RMS measured on the sample glass/gold/cobalt/gold (the intensity is in logarithmic scale).

From this XRRMS, we extract the specular reflectivity which is the horizontal section at $\omega = 0$. All other sections parallel with this one are off specular reflectivity allowing a more precise choice of $\delta(\theta)$. We will choose the one which corresponds to the disappearance of the interference fringes. Thus it practically represents the background and the corrected specular reflectivity of the background given by:

$$I_{\text{spec corr}} = I_{\text{spec}} - I_{\text{out spec}}$$

These two curves are represented on Fig. 6 as well as the corrected reflectivity.

The vertical sections represent the rocking curve which will be fitted by Gaussian profile in order to determine the percentage of the background. By applying the procedure described by F. Salah et al [6] we give a fraction of the background along the angular field in which the specular reflectivity was measured making it possible to obtain the corrected reflectivity of the background.

In comparison, Fig. 7 represents the normalized specular reflectivity extracted from XRRMS and that corrected of the background by both methods. We notice the two reflectivity curves corrected of the background by these methods are similar and a more important decrease in large angle respect to that not corrected. The corrected reflectivity of the background, estimated from off-set scan presents an improvement of the resolution of the interference fringes compared with that corrected from rocking curves.

Now, we will compare between the reflectivity corrected by the two methods extracted from XRRMS and those measured classically (according to the procedure described in [6]). Corrected specular reflectivity extracted from XRRMS and that measured classi-

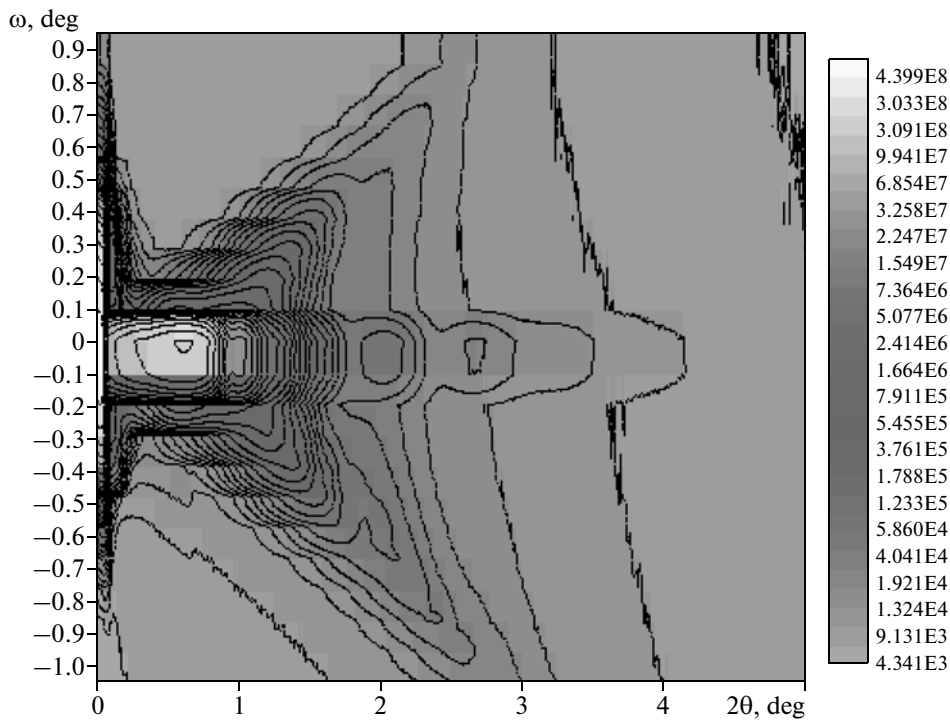


Fig. 5. X-ray reflectivity RMS measured on the sample glass/gold/cobalt/gold, the intensity is in logarithmic scale.

cally by off-set scan and rocking curve method are represented respectively in Fig. 8.

As shown in these figures, a better subtraction of the background by measuring a XRRMS is obtained because $\delta\theta$ is not an arbitrary parameter but it is much more precise considering the great choice of off spec-

ular reflectivity. The determination of the fraction of the background starting from the rocking curves extracted from XRRMS is also more precise because their number is much larger.

Geometrical corrections in the region of the plateau of total external reflection have also been em-

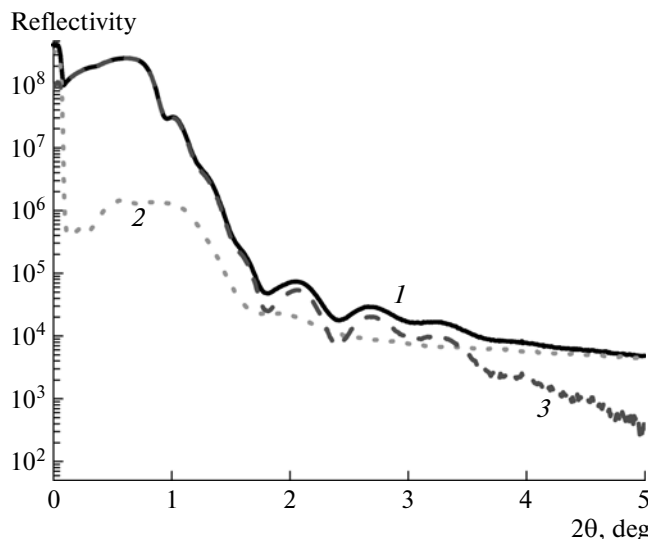


Fig. 6. Specular (1) and off specular (2) reflectivity of the sample glass/gold/cobalt/gold extracted from XRRMS. The correct reflectivity of the background is also represented (3).

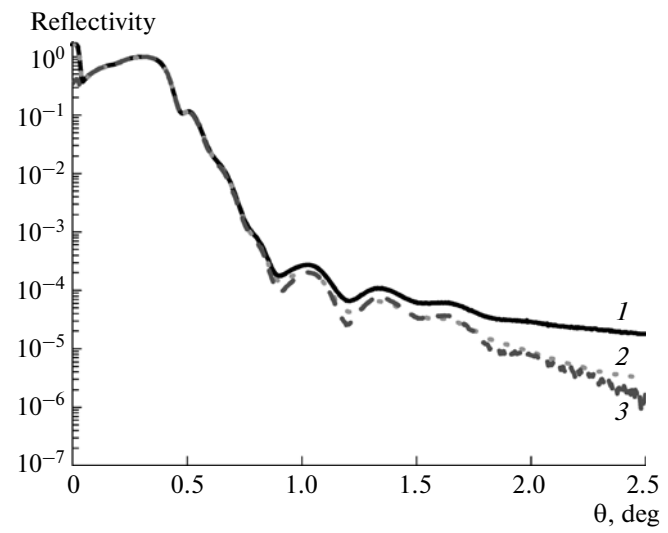


Fig. 7. Specular reflectivity (1) of the sample glass/gold/cobalt/gold extracted from XRRMS and those corrected of the background by off-set scan method (2) and by rocking curve method (3).

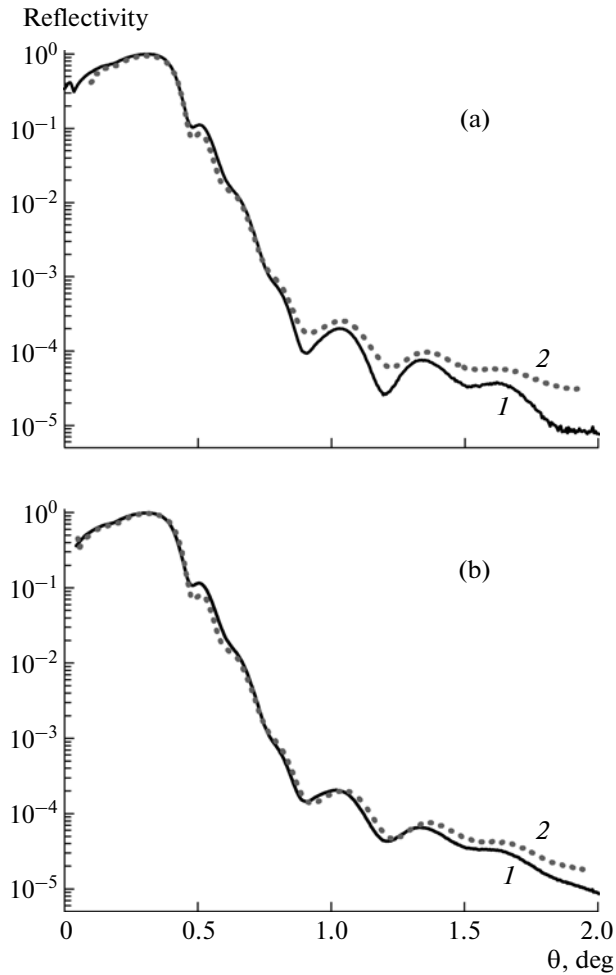


Fig. 8. Corrected specular reflectivity of the sample glass/gold/cobalt/gold extracted from XRRMS (1) and that measured classically (2) by off-set scan method (a) and by rocking curve method (b).

ployed as described in [6]. These authors explain in detail this footprint correction. Usually data fitting programs will not allow the application of such a correction to the calculated reflectivity, so that the inverse correction should be applied to the experimental curve.

4. DATA ANALYSIS AND COMPARISON

The analysis of raw specular reflectivity extracted from XRRMS and those corrected by two different methods has been carried out by non-linear least-squares fitting using Parrat's recursive relation [11]. Data fitting was performed with the paratt32 program [12]. For this method, the thin film is divided into a small number of parallel sub-layers, for each of which parameters such as the scattering density, thickness

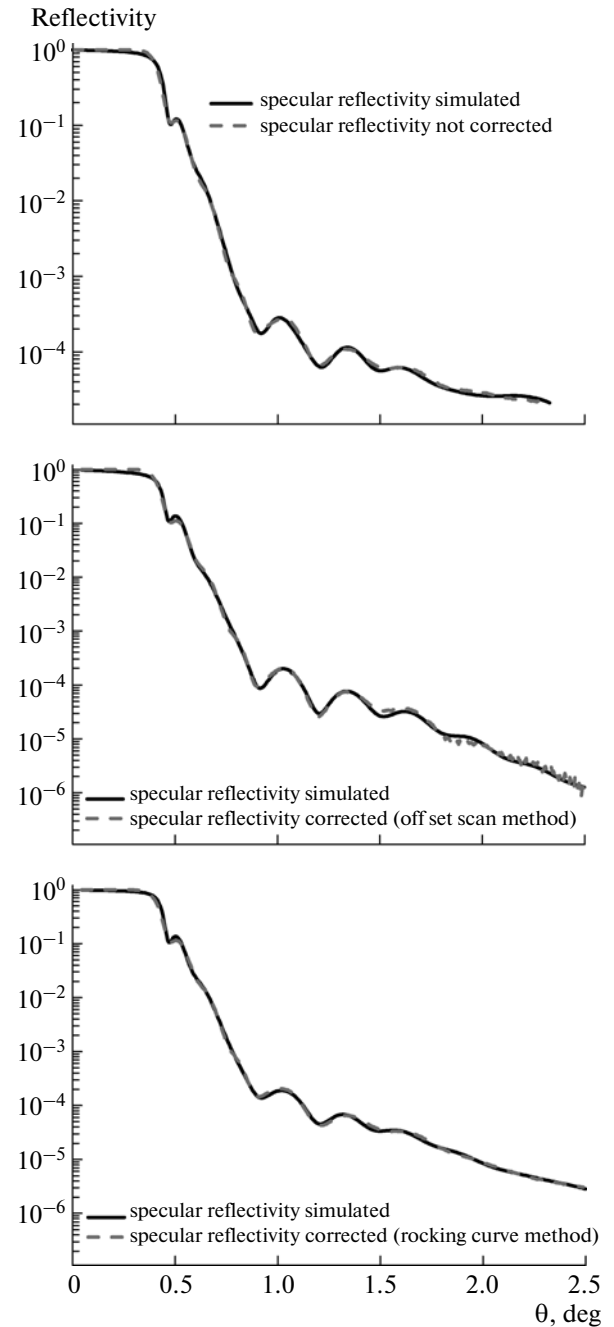


Fig. 9. Raw and corrected specular reflectivity of the sample glass/gold/cobalt/gold extracted from XRRMS with their best fits.

and interfacial roughness can be carried until a cost function is minimized.

Specular X-ray reflectivity is used in particular to probe the electronic density profile along the normal of the surface. It will be designated as the scattering-length density (SLD) profile $\rho(z)$ in units of \AA^{-2} . The relation between $\rho(z)$ and the electronic density $\rho_e(z)$

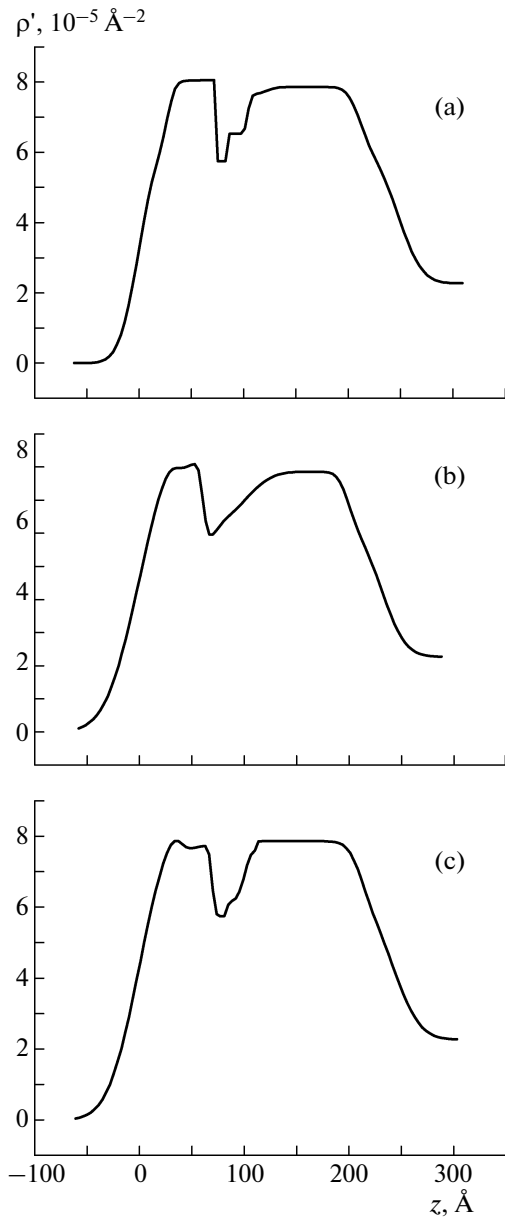


Fig. 10. Scattering length density profiles calculated from the best fit parameters to the reflectivity: (a) not corrected and corrected of background by; (b) off set scan method; (c) rocking curve method.

is $\rho(z) = \rho_0 \rho_e(z) = \rho'(z) + i\rho''(z)$, where r_0 is the Thomson scattering length of the electron.

As is well known, the chemical comparison should be known in order to calculate the mass density from the SLD or the electronic density; for X-ray case, the conversion formula is:

$$\rho_e = N_A \rho_m \frac{\sum_j c_j (z_j + f'_j + i f''_j)}{\sum_j c_j A_j}.$$

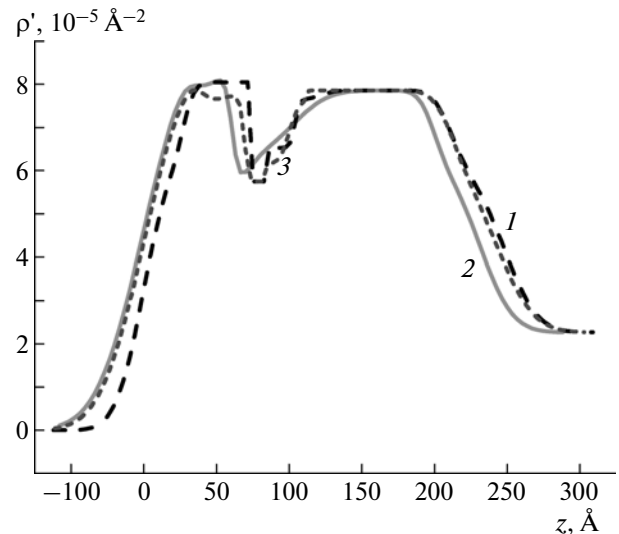


Fig. 11. Scattering length density profiles calculated from the best fit parameters to the reflectivity not corrected (1) and corrected of background by the two methods: off-set scan (2) and rocking curve (3).

Here N_A is Avogadro's number; ρ_m the mass density; z_j is the number of electrons of element j ; A_j is the atomic weight of electron j ; c_j is the molar fraction of element j and f'_j , f''_j are the anomalous dispersion corrections of element j .

Figure 9 gives the raw specular reflectivity and those corrected of the background estimated by two methods with their best fits. The scattering length density profiles calculated from the best fit parameters are shown in Fig. 10. The best fit of raw and corrected specular reflectivity are obtained by seven sub-layer models.

The fit structural parameter results are presented in table. The scattering length density profiles calculated from the best fit parameters to the not corrected and corrected background reflectivity curves by the two methods are represented in Fig. 11. We notice a variation of interfacial roughness of first sub-layer on a depth about 110 Å after a more precise adjustment of different sub-layer thickness.

For sub-layers 2, 6 and 7, we can verify the report ρ''/ρ' is in order of 0.101 which is practically equal to the bulk gold report (≈ 0.102) but for sub-layer 1, this report differs, probably due to the irregularities at air/gold interface. The report ρ''/ρ' of sub-layers 3 and 4 (≈ 0.147) is equal to that of bulk cobalt. However, we note the mass density of sub-layer 5 exceeds that of bulk cobalt in the case of not corrected and corrected by rocking curve method.

The total thickness of the cobalt sub-layer (3, 4 and 5) obtained from the fit of corrected reflectivity by the

Fit parameters results for reflectivity

	Thickness D , Å	ρ' , 10^{-5} Å $^{-2}$	ρ'' , 10^{-6} Å $^{-2}$	Roughness σ , Å	ρ_m , g · cm $^{-3}$
Not corrected of background					
Sub-layer 1	27.62	6.501	0.7176	15.077	10.11
Sub-layer 2	44.61	8.049	8.371	5.593	12.23
Sub-layer 3	11.15	5.75	8.44	0.005	8.10
Sub-layer 4	20.65	6.19	8.867	0.002	8.72
Sub-layer 5	17.21	7.629	11.25	2.429	10.74
Sub-layer 6	89.31	7.86	7.99	8.181	12.23
Sub-layer 7	37.03	6.162	6.817	9.552	9.59
Glass		2.27	0.3088	18.037	2.65
Corrected of background by off-set scan method					
Sub-layer 1	34.9	9.223	4.651	25.47	14.35
Sub-layer 2	25.66	8.29	8.3	7.1	12.90
Sub-layer 3	12.82	5.753	8.44	3.555	8.10
Sub-layer 4	13.54	6.18	9.10	7.226	8.71
Sub-layer 5	15.28	6.15	9.124	10.792	8.67
Sub-layer 6	96.7	7.863	7.99	19.062	12.91
Sub-layer 7	31.73	6.35	6.425	8.041	9.87
Glass		2.27	0.3088	18.091	2.65
Corrected of background by rocking curve method					
Sub-layer 1	39.48	8.69	1.867	23.582	13.52
Sub-layer 2	29.69	7.77	7.89	6.057	12.90
Sub-layer 3	15.09	5.75	8.44	2.407	8.10
Sub-layer 4	15.96	6.16	9.06	0.485	8.68
Sub-layer 5	10.4	7.65	11.24	5.317	10.78
Sub-layer 6	100.37	7.86	7.99	0.1	12.23
Sub-layer 7	31.19	6.35	6.44	9.991	9.88
Glass		2.27	0.3088	20.309	2.65

two methods is very near to that measured by quartz microbalance (≈ 40 Å). So the background as determined from the off-set scans method is expected to be more accurate.

5. CONCLUSIONS

Data reduction procedures in X-ray reflectivity are not very complicated to apply if the geometry and the conditions of the experiment are well known. The measurement of X-ray reflectivity reciprocal space mapping (XRRSM) has allowed to determine a precise contribution of background to the true reflectivity

signal. The advantage of XRRSM is that there is not an arbitrary $\delta\theta$ parameter to choose and the number of the rocking curves is much larger compared with traditional reflectivity measurement, but the total time of measurement is longer.

In order to compare the two background subtraction methods, a quantitative data analysis of layer thickness and interface roughness parameters was carried out by fitting extracted specular reflectivity from XRRMS with the paratt32 program. The comparison between the fit structural parameters results shows a more precise determination of background contribution by off-set scan method and as a consequence

thickness and roughness parameters will be deduced more exactly.

REFERENCES

1. Zhou, X.L., Chen, S.H., *Phys. Rep.*, 1995, vol. 257, p. 223.
2. Lu, J.R., Lee, E.M., Thomas, R.K., *Acta Cryst.*, 1996, vol. A52, p. 11.
3. Daillant, J., Gibaud, A., editors, *X-ray and Neutron Reflectivity: Principles and Applications*, Berlin: Springer, 1999. P. 114.
4. Als-Nielsen, J., McMorrow, D., *Elements of Modern X-ray Physics*, Chichester: Wiley, 1999.
5. Hill, R.J., in *The Rietveld Method*, Young, R.A., Ed., Oxford University Press, 1996. p. 61.
6. Salah, F., Harzallah, B., van der Lee, A., *J. Appl. Cryst.*, 2007, vol. 40, p. 813.
7. Fewster, P., *Semicond. Sci. Technol.*, 1993, vol. 8, p. 1915.
8. Itoh, N., Okamoto, K., *J. Appl. Phys.*, 1988, vol. 63, p. 1486.
9. Holz, T., Dietsch, R., Mai, H., Brügemann, L., *Adv. X-Ray Anal.*, 2000, vol. 43, p. 212.
10. Boulle, A., Guinebretière, R., Masson, O., et al., *Applied Surface Science*, 2006, vol. 253, p. 95.
11. Parrat, L.G., *Phys. Rev.*, 1954, vol. 95, p. 359.
12. Braun, C., *Paratt32 program for reflectivity analysis*, Berlin: HMI, 1997.